Vibrational-Rotational Laser Action in Carbon Monoxide

C. K. N. PATEL
Bell Telephone Laboratories, Murray Hill, New Jersey
(Received 23 August 1965)

In this paper we give details of the laser action on rotational transitions of 10-9, 9-8, 8-7, 7-6, and 6-5 vibrational bands belonging to the ground electronic state ($X^1\Sigma^+$) of CO. Laser action is produced in a low-pressure CO pulsed discharge. A comparison between the measured laser wavelengths (accuracy of ± 0.5 Å at 5.0–5.4 μ) and wavelengths calculated from available molecular constants of CO shows that a small correction in the vibrational constants may be necessary. A generalized treatment of optical gain on vibrational-rotational transitions is given and it is seen that it is advantageous to operate these lasers at as low a temperature as possible for production of maximum gain. An attempt is made to analyze the excitation mechanisms responsible for these laser transitions. It is seen that the excitation processes, under pulsed operation, have to be complicated and time-dependent in order to be able to duplicate theoretically the time dependence observed for the laser power output. It is shown that under the conditions of very selective excitation of a particular vibrational level, it should be possible to obtain cw laser oscillation on some P-branch vibrational-rotational transitions.

I. INTRODUCTION

INFRARED emission and absorption spectra of CO have been the subject of many investigations because of their importance as a diagnostic tool in the experiments involving flames, heat transfer during combustion, etc. The vibrational-rotational spectra belonging to the $X^1\Sigma^+$ state (ground electronic state) of CO have been studied[1–6] in spontaneous emission and absorption up to vibrational quantum number $v=6$. Very accurate determinations of the 4-3, 3-2, 2-1, and 1-0 vibrational-rotational band transitions reported in the works cited above have resulted in reliable and accurate determinations of the molecular constants of CO. Since the experiments so far have been carried out only for $v\leq 6$, the molecular constants were so adjusted that the measured and calculated wavelengths of the vibrational-rotational transitions agreed well for $v\leq 6$. In either spontaneous emission or in absorption studies, the typical CO pressures (or, in flame-emission studies, the $CO+O_2$ pressures) are typically in the region of several hundred Torr. This high pressure results in broadening (and frequency shift towards red) of the emission or absorption line due to collision effects (Lorentz broadening and Holtsmark broadening). Recently, spontaneous emission on 4-3, 3-2, 2-1, and 1-0 vibrational-rotational transitions of CO has been reported[7] in a scheme where excitation of CO molecules takes place because of the transfer of vibrational energy of N_2^* ($v=1, 2, \cdots$) (nitrogen molecules excited to various vibrational levels of their ground electronic state $X^1\Sigma_g^+$). Here the typical gas pressures are in the region of a few Torr.

In this paper we report laser action on a number of lines in the 5.0- to 5.4-μ region. These lines are identified[8] to be the P-branch rotational transitions belonging to the 10-9, 9-8, 8-7, 7-6, and the 6-5 vibrational bands of CO of $X^1\Sigma^+$ state. Laser action occurs in a pulsed dc discharge in low-pressure CO. Previously, laser action on the angstrom-band electronic transitions has been reported[9] [in the visible and near infrared (IR) region]. The CO pressure was typically of the order of a fraction of a Torr and thus, in comparison with the previous determinations and observations of the ground electronic state vibrational-rotational spectra in either absorption spectroscopy or flame emission spectroscopy, the present results should be considerably less affected by pressure-dependent frequency shifts and broadening of the transitions. And, in addition, the high power output ($\sim$100 μW on the stronger laser transitions) together with its high directionality and coherence properties should allow extremely careful and accurate determinations of the laser wavelengths; indeed, this paper seems to be the first one to report the observation of the vibrational-rotational transitions of the $X^1\Sigma^+$ state of CO for $v>6$ in any kind of spectroscopy (absorption, spontaneous emission, or stimulated emission spectroscopy).[10] With the strong optical power on a number of transitions in the 5.0- to 5.4-μ region, it should be possible to measure these lines with improved precision using interferometric techniques. This may then yield improved wavelength standards for spectroscopy in this region.

In the next section we describe briefly the experimental technique and apparatus used in the present

[1] W. S. Benedict, R. Herman, G. E. Moore, and S. Silverman, Astrophys. J. **135**, 277 (1962) and references cited herein.
[2] E. K. Plyler, W. S. Benedict, and S. Silverman, J. Chem. Phys. **20**, 175 (1952).
[3] K. E. McCulloh and G. Glockler, Phys. Rev. **89**, 145 (1953).
[4] R. T. Lageman, H. H. Nielsen, and F. P. Dickey, Phys. Rev. **72**, 284 (1947); G. Herzberg and K. N. Rao, J. Chem. Phys. **17**, 1099 (1949).
[5] S. S. Penner, *Quantitative Molecular Spectroscopy and Gas Emissivities* (Addison-Wesley Publishing Company, Inc., Reading, Massachusetts, 1959).
[6] L. Goldberg and E. A. Müller, Astrophys. J. **118**, 397 (1953).
[7] F. Legay and N. Legay-Sommaire, Compt. Rend. **257**, 2644 (1963); N. Legay-Sommaire and F. Legay, J. Phys. Radium **25**, 917 (1964).
[8] C. K. N. Patel and R. J. Kerl, Appl. Phys. Letters **5**, 81 (1964).
[9] L. E. S. Mathias and J. T. Parker, Phys. Letters **7**, 194 (1964).
[10] In our first communication on this subject (Ref. 8) we had erroneously claimed that none of the vibrational-rotational transitions for $v>5$ had been observed before. This now has been corrected to read $v>6$.

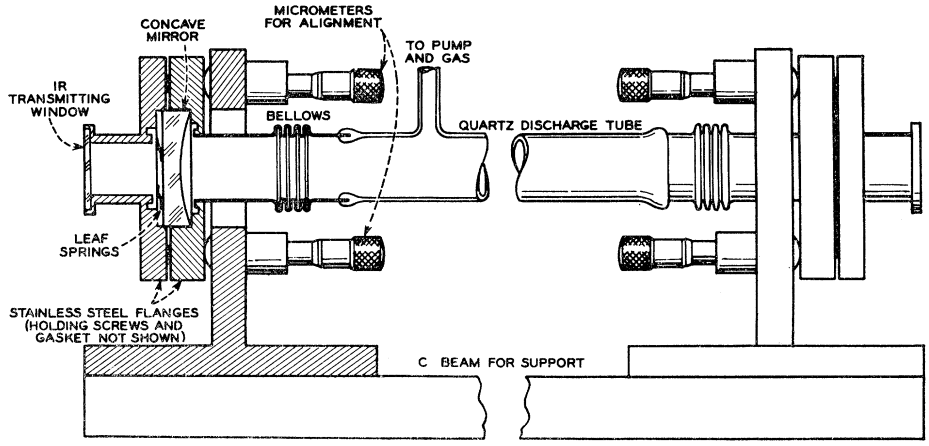

FIG. 1. Sketch of laser used in investigation of CO vibrational-rotational laser transitions.

investigation. Section III presents the experimental results and a discussion on the comparison of the measured and the calculated values of the frequencies for the laser transitions. In Sec. IV we give a theoretical interpretation of the laser oscillation on the P-branch rotational transitions (of the vibrational bands of the $X^1\Sigma^+$ ground electronic state of CO) by carrying out an analysis similar to that reported earlier for the case of CO_2 (Ref. 11). The analysis is generalized to include possible vibrational-rotational interaction effects in the matrix elements for the various vibrational-rotational transitions. Section V is a detailed discussion of excitation processes responsible for the laser action on the vibrational-rotational transitions of CO and also gives other possible means for obtaining an effective excitation. In case of a pure CO discharge, it is unlikely that the excitation of CO molecules to the vibrational levels of the ground electronic state arises because of direct excitation from ground vibrational level. The most likely source of excitation is through a cascade from higher lying electronic states or through a compound state of CO lying at 2.2 eV as reported by Schulz.[12] A detailed discussion of time-dependence analysis of the laser output is given. It is seen that the CO vibrational-rotational laser transitions are of cascade nature, a fact borne out very dramatically from the time dependence data. From assumed excitation conditions, we have tried to obtain the population inversions as a function of time. It appears that the excitation conditions will have to be very complicated and time-dependent in order to calculate the actual time dependence of laser output to match the experimentally observed results.

From the lifetime considerations, it can be seen that, under cw operating conditions, no inversion between total population densities of two vibrational levels can occur in CO. However, we show that with an extremely selective excitation of only one vibrational level, some of the P branch rotational transitions can have cw population inversions, and possibilities of cw operation of CO vibrational-rotational transitions cannot be neglected. The conclusion that selective excitation is necessary for cw operation of the CO vibrational-rotational laser is also applicable to other diatomic molecules in which the vibrational-rotational transitions have been made to oscillate. It can be seen that in the case of diatomic molecules, the problem of obtaining cw oscillation on the vibrational-rotational transitions of the ground electronic state simplifies considerably if strong collisional deactivation of certain vibrational levels is possible in addition to their radiative deactivation. This collisional deactivation has been found to be very slow in the case of CO.[13,14] Up to the present time, we have not been able to operate these CO vibrational-rotational transitions under cw conditions.

II. EXPERIMENTAL ARRANGEMENT

Figure 1 shows a sketch of the laser used in the investigation of laser action in CO. In principle it is similar to those used in other far infrared laser investigations described earlier.[15] The discharge tube was made out of quartz and was 47 mm i.d. and 480 cm long. The optical cavity was formed by two concave mirrors having a 5-m radius of curvature spaced 510 cm apart to form a near confocal cavity.[16] The silicon mirrors were coated with vacuum-deposited gold for high reflectivity in the 5-μ region of the infrared spectrum.[17] As with our earlier experiments, the energy was coupled out of the optical resonator through a 0.030-in. diam uncoated

[11] C. K. N. Patel, Phys. Rev. Letters **12**, 588 (1964); Phys. Rev. **136**, 1187 (1964).
[12] G. J. Schulz, Phys. Rev. **135**, A988 (1964).
[13] R. C. Millikan, J. Chem. Phys. **38**, 2855 (1963); **39**, 3209 (1963).
[14] V. N. Kondrat'ev, *Chemical Kinetics of Gas Reactions* (Addison-Wesley Publishing Company, Inc., Reading, Massachusetts, 1964).
[15] W. L. Faust, R. A. McFarlane, C. K. N. Patel, and C. G. B. Garrett, Phys. Rev. **133**, A1476 (1964).
[16] G. D. Boyd and H. Kogelnik, B. S. T. J. **41**, 1347 (1962).
[17] Vacuum deposited silver, aluminum and gold have high reflectivity in the infrared. Silver has slightly higher reflectivity than gold or aluminum, but it is considerably less durable. For quantitative values of reflectivity of silver, aluminum, and gold refer to J. M. Bennett and E. J. Ashley, Appl. Opt. **4**, 221 (1965).

TABLE I. Measured and calculated wavelengths and frequencies of CO pulsed laser transitions together with identifications of the laser lines, delay for each band after the current pulse and the strongest laser transition in each vibrational band.

λ_{obs} (vac)	Identification Vibrational band	Transition	ν_{meas} (cm^{-1})	ν_{calc} (cm^{-1})[a]	Difference $\nu_{meas}-\nu_{calc}$ (cm^{-1})	Delay[b] (after the current pulse)	Remarks
5.03755	6-5	$P(7)$	1985.09	1985.09	0	Typically 60-70 μsec	Strongest transition in the 6-5 band, $P(11)$
5.04750		$P(8)$	1981.18	1981.18	0		
5.05755		$P(9)$	1977.24	1977.24	0		
5.06773		$P(10)$	1973.27	1973.26	0.01		
5.07807		$P(11)$	1969.25	1969.25	0		
5.08845		$P(12)$	1965.23	1965.20	0.03		
5.09905		$P(13)$	1961.15	1961.12	0.03		
5.10985		$P(14)$	1957.00	1957.01	−0.01		
5.10410	7-6	$P(7)$	1959.21	1959.19	0.02	Typically 70-80 μsec	Strongest transition in the 7-6 band, $P(11)$
5.11418		$P(8)$	1955.35	1955.32	0.03		
5.12445		$P(9)$	1951.43	1951.41	0.02		
5.13485		$P(10)$	1947.48	1947.46	0.02		
5.14530		$P(11)$	1943.52	1943.49	0.03		
5.15595		$P(12)$	1939.51	1939.48	0.03		
5.16666		$P(13)$	1935.48	1935.43	0.05		
5.17765		$P(14)$	1931.38	1931.36	0.02		
5.18865		$P(15)$	1927.28	1927.25	0.03		
5.17220	8-7	$P(7)$	1933.41	1933.36	0.05	Typically 100 μsec	Strongest transition in the 8-7 band, $P(11)$
5.18250		$P(8)$	1929.57	1929.52	0.05		
5.19290		$P(9)$	1925.71	1925.65	0.06		
5.20345		$P(10)$	1921.80	1921.74	0.06		
5.21410		$P(11)$	1917.87	1917.80	0.07		
5.22498		$P(12)$	1913.88	1913.82	0.06		
5.23600		$P(13)$	1909.85	1909.81	0.04		
5.24710		$P(14)$	1905.81	1905.77	0.04		
5.24195	9-8	$P(7)$	1907.69	1907.60	0.09	Typically 150 μsec	Strongest transition in the 9-8 band, $P(10)$
5.25250		$P(8)$	1903.85	1903.79	0.06		
5.26310		$P(9)$	1900.02	1899.95	0.07		
5.27380		$P(10)$	1896.17	1896.08	0.09		
5.28465		$P(11)$	1892.27	1892.17	0.10		
5.29570		$P(12)$	1888.32	1888.23	0.09		
5.30695		$P(13)$	1884.32	1884.26	0.06		
5.31820		$P(14)$	1880.33	1880.25	0.08		
5.32415	10-9	$P(8)$	1878.23	1878.13	0.10	Typically 220 μsec	Strongest transition in the 10-9 band, $P(11)$
5.33490		$P(9)$	1874.45	1874.33	0.12		
5.34590		$P(10)$	1870.59	1870.49	0.10		
5.35695		$P(11)$	1866.73	1866.62	0.11		
5.36820		$P(12)$	1862.82	1862.72	0.10		
5.37950		$P(13)$	1858.91	1858.78	0.13		

[a] ν_{calc} obtained using constants obtained from Ref. 1 (see text also).
[b] Under the following experimental conditions: $P_{CO}=0.8$ Torr, I_{peak}(pulse) $=15$ A, V_{peak}(pulse) $=15$ kV.

aperture at the center of one of the mirrors. (See, for example, Ref. 18 for a description of this technique.) There were no wavelength selective devices inserted in the cavity (which as seen from Fig. 1 is enclosed in vacuum). Thus the optical loss in the cavity (and hence the optical Q of the cavity) at a given wavelength was determined only from (1) diffraction losses, (2) reflection losses at the mirrors and (3) transmission loss through the uncoated aperture at the center of the output mirror. The diffraction losses determine the long-wavelength low-loss limit for the operation of the cavity,[16] the transmission loss determines the short-wavelength limit,[19] and the reflection losses are relatively constant over the infrared region of wavelength.[17] Thus in the region of wavelength from 4 μ to 6 μ the cavity losses can be taken as constant and thus the strengths of various oscillation transitions will depend only upon their relative population inversions. This point will be further discussed in Sec. IV.

Typical carbon monoxide pressure in these experiments was about 0.8 Torr. (The CO used here was about 99.95% pure with CO_2 being the chief impurity.) 15-kV peak voltage and 15-A peak current, 1-μsec nominal-duration electrical pulses were used for obtaining the pulsed discharge in CO.

A liquid-nitrogen-cooled InSb photoconductor was used as the detector for the 5.0- to 5.4-μ radiation. The detector had an N.E.P. (noise equivalent power) of about 10^{-10} W/cps$^{1/2}$. The speed of response of the InSb photoconductive detector was judged to be about 1 μsec as determined from looking at the risetime of the

[18] C. K. N. Patel, W. L. Faust, R. A. McFarlane, and C. G. B. Garrett, Appl. Phys. Letters 4, 18 (1964).
[19] For a detailed discussion on this subject see Ref. 11.

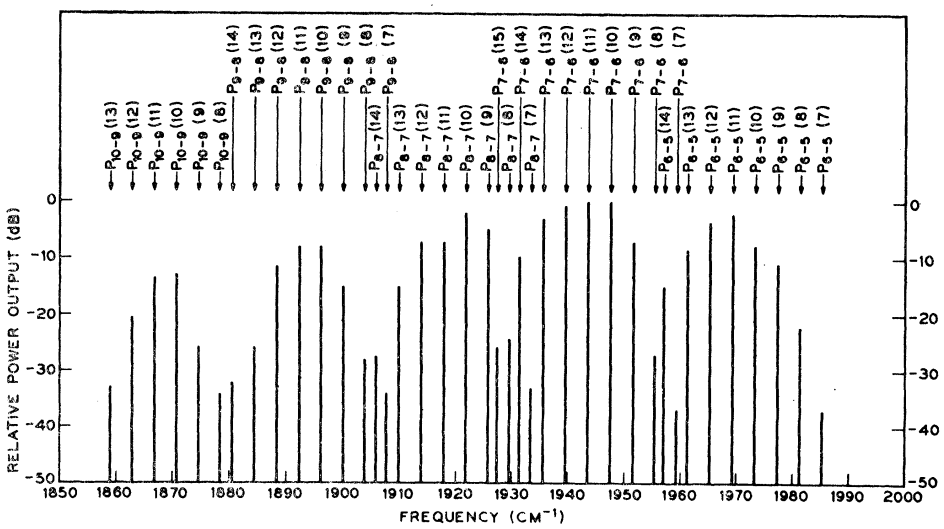

FIG. 2. Intensities of laser lines and identifications plotted against wavelength.

3.3922-μ laser radiation from a pulsed helium-neon laser. The output power (peak power output on the CO laser radiation being investigated here) measurements were carried out by calibrating the detector against a thermopile. Wavelength measurements were carried out using a 1-m Ebert scanning spectrometer equipped with a grating blazed at 6.0 μ. (Grating ruling was 63 mm high and 190 mm wide.) The spectrometer was calibrated against a helium-neon laser operating at 6328 Å (vacuum) in the eighth and the ninth orders of the grating. The wavelength measurements were carried out in vacuum by evacuating the spectrometer. The precision and accuracy of the wavelength measurements was judged to be about ± 0.5 Å (i.e., the frequency determination accuracy of about ± 0.02 cm^{-1}).

III. EXPERIMENTAL RESULTS AND DISCUSSION

Table I shows the experimental results on the measurements of the CO vibrational-rotational laser transitions. The laser lines are grouped according to the vibrational bands to which they have been identified as belonging. The measured wavelengths and frequencies are given in vacuum. The laser lines are identified as the P-branch rotational transitions belonging to the 10-9, 9-8, 8-7, 7-6, and 6-5, vibrational bands of the $X^1\Sigma^+$ ground electronic state of CO. In Table I we have also given the calculated values of frequency of the identified transitions as obtained from CO molecular constants reported by Benedict *et al.*[1] These are

(a) vibrational constants

$$\omega_e = 2169.830 \text{ cm}^{-1},$$
$$\omega_e x_e = 13.297 \text{ cm}^{-1},$$
$$\omega_e y_e = 0.0115 \text{ cm}^{-1};$$

(b) rotational constants

$$\beta_e = 1.93141 \text{ cm}^{-1},$$
$$\alpha = 0.017520 \text{ cm}^{-1},$$
$$\gamma = 2.96 \times 10^{-6} \text{ cm}^{-1},$$
$$D_e = 6.18 \times 10^{-6} \text{ cm}^{-1},$$
$$\beta = -1.76 \times 10^{-9} \text{ cm}^{-1}.$$

It has been shown in Ref. 1 that these constants are precise enough to allow us to calculate the transition frequencies for the vibrational-rotational transitions up to $v=6$. There are no previously reported measurements on the vibrational-rotational transitions for $v>6$ in any kind of spectroscopy. (There are, however, determinations of the $v>6$ vibrational levels as obtained from uv spectroscopy on the fourth positive band system of CO, i.e., on the $A^1\Pi \rightarrow X^1\Sigma^+$ band.[20]) We see from Table I that there are discrepancies between the measured and calculated values of frequencies. The difference between measured frequency and calculated frequency for the CO vibrational-rotational transitions ($\nu_{\text{meas}} - \nu_{\text{calc}}$) is within the experimental accuracy for the $v=6 \rightarrow v=5$ vibrational-rotational band. However, it can be seen that the difference $\nu_{\text{meas}} - \nu_{\text{calc}}$ increases as we go to higher vibrational bands. Table II gives the average difference for each one of the bands together with the scatter for

TABLE II. Average difference $\nu_{\text{meas}} - \nu_{\text{calc}}$ for each of the laser bands.

Vibrational band	Average difference[a] $\nu_{\text{meas}} - \nu_{\text{calc}}$ (cm^{-1})	Scatter (cm^{-1})
$6 \rightarrow 5$	+0.01	± 0.02
$7 \rightarrow 6$	+0.03	± 0.02
$8 \rightarrow 7$	+0.05	± 0.02
$9 \rightarrow 8$	+0.08	± 0.02
$10 \rightarrow 9$	+0.11	± 0.02

[a] Obtained from differences in Table I.

[20] D. N. Read, Phys. Rev. 46, 571 (1934).

each band. The scatter is seen to be within the claimed experimental accuracy and precision to which the wavelengths have been measured. It is felt from these observations that the rotational constants used in obtaining calculated values of frequency are perhaps accurate (since there is no well-defined trend in the differences for the rotational transitions within a vibrational band). But there is a significant trend in the differences in that all the rotational lines of the vibrational bands seen here are seen to shift in the same direction. This indicates that the vibrational constants given in Ref. 1, which have been successfully used for calculating the transition frequencies up to $v=6$ will have to be slightly modified in order to match the measured and calculated values of frequencies of the laser transitions belonging to the vibrational-rotational bands up to $v=10$. The change required is very small and is not attempted at the present time. In our first announcement of the CO vibrational-rotational laser transitions, we had used vibrational constants as given by McCulloh and Glockler[3] and rotational constants given by Plyler *et al.*[2] to calculate the frequencies of the transition for identification purposes. In that case it was seen that there was no significant trend in the differences for various vibrational bands, but within a band there was a regular trend in differences indicating inaccurate rotational constants. It is clear to see that since these laser transitions produce microwatts of power, it should be easy to make interferometric wavelength measurements to yield more precise values of frequencies and of molecular constants.

Under the experimental conditions of $P_{CO}\approx 0.8$ Torr, $V_{peak}(\text{pulse})\approx 15$ kV and $I_{peak}(\text{pulse})\approx 15$ A, we obtained the relative intensity data on the laser transitions. Figure 2 shows a plot of intensities of the laser lines as a function of wavelength. The laser transitions are shown as vertical lines with their heights corresponding to their intensities. The existence of five bands is immediately obvious. The intensities are given in dB below the strongest laser power output which was on the $P_{7-6}(11)$ transition. [The power output on $P_{7-6}(11)$ was ≈ 100 μW.] It should be pointed out that during this measurement, no attempt was made to adjust the cavity length for maximum power output on each individual transition. The Doppler width of the CO vibrational-rotational transitions around 5 μ is expected to be about 125 Mc/sec (assuming $T_{mol}\approx 400$°K) and the cavity longitudinal mode spacing about 30 Mc/sec. Hence the tuning of the cavity length will have a small effect on the laser output on any given transition. Thus, there are small discrepancies in the strongest rotational transition for each vibrational band as seen in Fig. 2 and as given in Table I. The data in Table I are more reliable since every care was taken to see that each transition power output was maximized with respect to the cavity tuning. The absence of cavity length tuning for the data in Fig. 2 also caused the intensities of the laser output on rotational transitions in each vibrational band not to decrease monotonically on either side of the strongest transition. (When proper care is taken to accomplish this, the power output on the rotational transitions away from the strongest on either side decreased monotonically.) But Fig. 2 is given to show what can be expected from a laser described in the text under normal conditions if no attempt is made to optimize each laser transition.

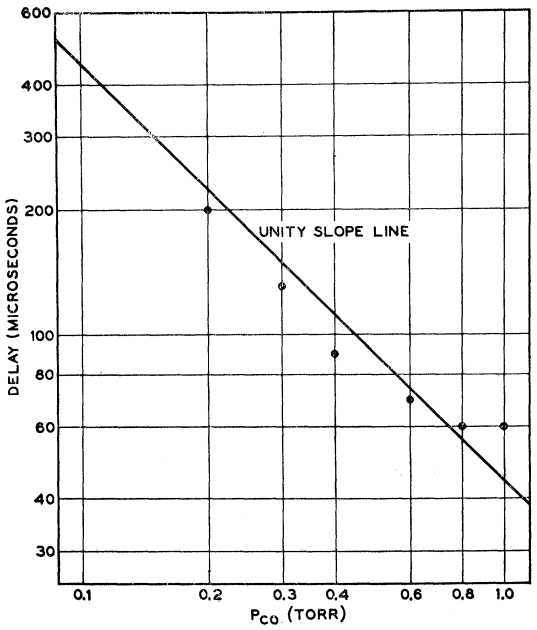

FIG. 3. Delay of laser output pulse on $P_{6-5}(11)$ transition (after the current pulse) as a function of CO pressure.

As mentioned a little earlier, the maximum laser power output of ≈ 100 μW was obtained on the $P_{7-6}(11)$ transition. It was seen, however, that this was not the maximum power which could be achieved with respect to the input pulse electrical power. No power saturation was seen and thus it is felt that the limitation on the power output at present perhaps lies with the limit of the power output from the electrical pulser.

Table I also shows the delay of the laser output pulse after the current excitation pulse. The delay was seen to be approximately constant for all the rotational transitions within a vibrational band, but the delay was different for different vibrational bands. The delay was a function of CO pressure and the pulse electrical power input to the discharge. The delay times given in Table I are under the conditions of optimum CO pressure for maximum optical power output when the electrical pulser was delivering its peak power output of 225 kW, i.e., $V_{peak}(\text{pulse})=15$ kV and $I_{peak}(\text{pulse})=15$ amps. In general, the delay decreased with increasing pressure and with increasing power input. Figure 3 shows the delay for the power output on $P_{6-5}(11)$ transition as a function of CO pressure when $I_{input}(\text{pulse})\approx 15$ A. On the log-log plot we have in addition shown a unity slope line for comparison. It was

also seen that increasing the cavity losses by detuning the cavity mirror alignment, for example, resulted in increased delay, indicating that the delay is cause by some slow excitation mechanism which builds up the population densities of various vibrational levels until enough inversion has been established to have optical gain exceed the optical losses for oscillation. This aspect will be further discussed in the section mechanisms.

It can be seen from Table I that all of the laser transitions reported in Table I are of cascade nature.[21] For example, two of the cascade chains can be written as follows:

$$\begin{bmatrix} v=10 \\ J=8 \end{bmatrix} \xrightarrow[P_{10\text{-}9}(9)]{} \begin{bmatrix} v=9 \\ J=9 \end{bmatrix} \xrightarrow[P_{9\text{-}8}(10)]{} \begin{bmatrix} v=8 \\ J=10 \end{bmatrix} \xrightarrow[P_{8\text{-}7}(11)]{} \begin{bmatrix} v=7 \\ J=11 \end{bmatrix} \xrightarrow[P_{7\text{-}6}(12)]{} \begin{bmatrix} v=6 \\ J=12 \end{bmatrix} \xrightarrow[P_{6\text{-}5}(13)]{} \begin{bmatrix} v=5 \\ J=13 \end{bmatrix}, \tag{1}$$

$$\begin{bmatrix} v=9 \\ J=8 \end{bmatrix} \xrightarrow[P_{9\text{-}8}(9)]{} \begin{bmatrix} v=8 \\ J=9 \end{bmatrix} \xrightarrow[P_{8\text{-}7}(10)]{} \begin{bmatrix} v=7 \\ J=10 \end{bmatrix} \xrightarrow[P_{7\text{-}6}(11)]{} \begin{bmatrix} v=6 \\ J=11 \end{bmatrix} \xrightarrow[P_{6\text{-}5}(12)]{} \begin{bmatrix} v=5 \\ J=12 \end{bmatrix}, \tag{2}$$

where the laser transitions are indicated below the arrows.

A time dependence study of the various members of a chain like those shown in Eqs. (1) and (2) shows the cascade nature of the transitions very clearly. In Fig. 4, we have shown the laser output pulses for the four cascade transitions represented in Eq. (2). For each one of the oscillograms, the excitation current pulse occurs at the beginning of the trace. (On some of the oscillograms, the stray pickup of the current pulse is seen as a sharp spike at the left-hand corners.) In the trace (d), the $P_{6\text{-}5}(12)$ transition at 5.08845 μ starts oscillating after a delay of about 60 μsec (characteristic delay for all the other 6-5 band rotational laser transitions). No other bands have started oscillating yet. Owing to the increased radiative decay rate of the $v=6$ vibrational band (due to addition of stimulated emission decay), the population density of the $v=6$ vibrational level decays more rapidly than that of the $v=7$ level, and soon population inversion is established between the $v=7$ and $v=6$ vibrational levels. Thus in trace (c) we see that $P_{7\text{-}6}(11)$ breaks into oscillation after a delay of about 70 μsec (typical delay for other 7-6 band vibrational-rotational transitions). With the start of stimulated emission on the 7-6 vibrational-rotational transitions, we observe two effects.

(1) Increase in supply rate of molecules to the $v=6$ vibrational level. This shows up as a sharp increase in the laser power output on the $P_{6\text{-}5}(12)$ transition in trace (d) as expected at $t=70$ μsec.

(2) Increase in the total decay rate of molecules in the $v=7$ level causes inversion to be established between the $v=8$ and $v=7$ vibrational levels after a delay of about 100 μsec.

Thus, in trace (b) we see that $P_{8\text{-}7}(10)$ starts oscillating at $t=100$ μsec which is typical for other rotational transitions belonging to the $v=8 \rightarrow v=7$ vibrational band. This laser oscillation again increases the population density of the upper laser level for 7-6 vibrational-rotational transitions. This causes an increase in the laser power output on the $P_{7\text{-}6}(11)$ transition as seen in trace (c) at $t \approx 100$ μsec. This in turn results in an increase in the laser power output on $v=7 \rightarrow v=6$ vibrational-rotational transitions as seen in trace (d) for the $P_{6\text{-}5}(12)$ transition at $t \approx 100$ μsec. The laser oscillation on the 8-7 transition causes an increase in the decay rate for the $v=8$ vibrational level resulting in laser oscillation on $v=9 \rightarrow v=8$ vibrational-rotational transitions. From trace (a) in Fig. (4) we see that $P_{9\text{-}8}(9)$ starts oscillating after a delay of about 150 μsec. This causes an increase

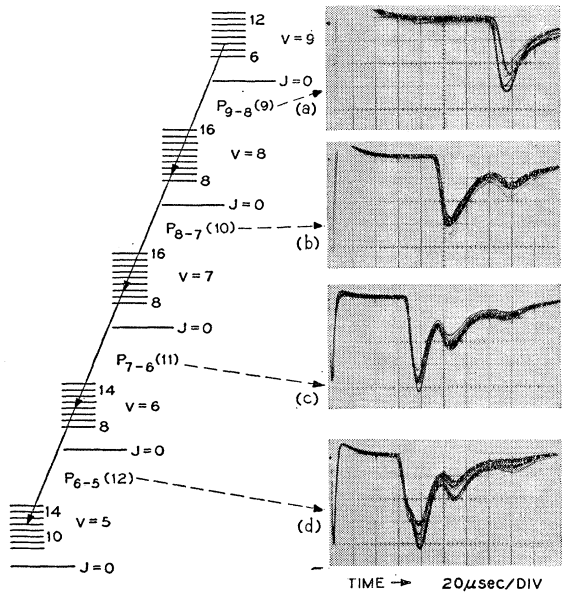

FIG. 4. Laser pulses showing cascade nature of CO laser transitions described in Eq. (2): (a) $P_{9\text{-}8}(9)$ at 5.26310 μ, (b) $P_{8\text{-}7}(10)$ at 5.20345 μ, (c) $P_{7\text{-}6}(11)$ at 5.14530 μ, and (d) $P_{6\text{-}5}(12)$ at 5.08845 μ. (Energy-level diagram, not to scale, is shown on the left. In each of the oscilloscope traces, the current pulse occurs at the left-hand edge.)

[21] R. A. McFarlane, W. L. Faust, C. K. N. Patel, and C. G. B. Garrett, *Quantum Electronics III*, edited by P. Grivet and N. Bloembergen (Columbia University Press, New York, 1964), pp. 573–586; R. Cagnard, R. der Agobian, R. Erchard, and J. Otto, Compt. Rend. **257**, 1044 (1963); R. der Agobian, J. Otto, R. Erchard, and R. Cagnard, *ibid.* **257**, 3844 (1963).

in the laser output on the laser transitions between the $v=8$, 7, 6, and 5 vibrational levels. We see this very graphically in trace (b) for $P_{8\text{-}7}(10)$, trace (c) for $P_{7\text{-}6}(11)$ and trace (d) for $P_{6\text{-}5}(12)$ transitions in that an increase in the laser power output occurs at $t\approx 150\,\mu$sec. This cascading effect is seen for the cascade chain in Eq. (1) and all other cascade chains of laser transitions from CO vibrational-rotational laser. It is seen, thus, that the molecules excited to the various vibrational levels cascade from one vibrational level to the one below producing laser action at a number of different wavelengths. A theoretical analysis with assumed initial excitation conditions to match the observed time dependence of the vibrational-rotational laser transitions such as those shown in Fig. 4 will follow in the last section.

IV. THEORETICAL DISCUSSION OF GAIN

In Ref. 11 we had obtained expressions for optical gain on P- and R-branch rotational transitions of the 00°1-10°1 and 00°1-02°0 vibrational bands of CO_2. These expressions are in general valid for diatomic molecules also. We will not go through the complete rederivation but will give the final expressions for gain in generalized forms.

Using the following notation: $\alpha_{vJv'J'}$, optical gain at the center of the $J\rightarrow J'$ rotational transition of the $v\rightarrow v'$ vibrational band (the transition is assumed to be Doppler broadened); $\lambda_{vJv'J'}$, center wavelength of the transition $v_J\rightarrow v'_{J'}$; $\nu_{vJv'J'}$, center frequency of the transition $v_J\rightarrow v'_{J'}$; and c, velocity of light;

$$K_{vv'}S_J\mathfrak{F}_{vJv'J'}=|R_{vJv'J'}|^2$$
$$=\text{matrix element for the transition } v_J\rightarrow v'_{J'}$$

(see Ref. 22). $K_{vv'}$ is the vibrational contribution to the matrix element[23] (J-independent); $S_J\mathfrak{F}_{vJv'J'}$ is the rotational contribution to the matrix element; $\mathfrak{F}_{vJv'J'}$ is the vibrational-rotational interaction factor for the $v_J\rightarrow v'_{J'}$ transition; k is the Boltzmann constant; T_{rot} is the rotational equilibrium temperature (assumed to be the same for both v and v' vibrational levels); T_{mol} is the molecular temperature; M is the molecular mass; N_v, $N_{v'}$ is the total population densities in the v and v' vibrational levels, respectively; B_v, $B_{v'}$ is the rotational constants for levels v and v', respectively; and $F(J)$ is the energy of Jth rotational level from 0th level and equals $BJ(J+1)-DJ^2(J+1)^2$, with

$$D\ll B.$$

Gain at frequencies other than the transition center is given by

$$\alpha_{vJv'J'}(\nu)=\alpha_{vJv'J'}\exp[-(\nu-\nu_{vJv'J'}/\Delta\nu_D\ln 2)^2], \quad (3)$$

where

$$\Delta\nu_D=\text{Doppler width of the transition}$$
$$=(2\nu_{vJv'J'}/c)[(2kT_{\text{mol}}/M)\ln 2]^{1/2}. \quad (4)$$

Hence from Ref. 12, on generalizing, we obtain

$$\alpha_{vJv'J'}=\frac{8\pi^3c^4K_{vv'}}{3kT_{\text{rot}}(2\pi kT_{\text{mol}}/M)^{1/2}}S_J\mathfrak{F}_{vJv'J'}\left[N_vB_v\exp\left(-F_v(J)\frac{hc}{kT_{\text{rot}}}\right)-N_{v'}B_{v'}\exp\left(-F_{v'}(J')\frac{hc}{kT_{\text{rot}}}\right)\right]. \quad (5)$$

The expression is now very general and includes the possible effect of vibrational-rotational interaction on the matrix element by introducing the factors $\mathfrak{F}_{vJv'J'}$. This interaction factor is unity for a rigid rotator.[22] (In our earlier analysis[12] of CO_2, we had tacitly substituted $\mathfrak{F}_{vJv'J\pm1}=1$ which is appropriate for the analysis of the 00°1-10°0 and 00°1-02°0 vibrational-rotational bands of CO_2.)

Now let us apply this expression to our discussion of laser action on the vibrational-rotational transitions of the $X^1\Sigma^+$ state of CO. Here the only transitions allowed are $v_J\rightarrow v'_{J\pm1}$ and $\mathfrak{F}_{vJv'J\pm1}\approx 1$. Thus, we obtain

$$\alpha_{vJv'J\pm1}=\frac{8\pi^3c^4K_{vv'}}{3kT_{\text{rot}}(2\pi kT_{\text{mol}}/M)^{1/2}}S_J\left[N_vB_v\exp\left(-F_v(J)\frac{hc}{kT_{\text{rot}}}\right)-N_{v'}B_{v'}\exp\left(-F_{v'}(J\pm1)\frac{hc}{kT_{\text{rot}}}\right)\right]. \quad (6)$$

With the substitutions

$$T\approx T_{\text{rot}}\approx T_{\text{mol}},$$
$$S_J=J+1 \quad \text{for } P\text{-branch rotational transitions},$$

and

$$S_J=J \quad \text{for } R\text{-branch rotational transitions},$$

where J is the rotational quantum number of the *upper level*. We obtain

(a) For P-branch rotational transitions, i.e., for $P(J+1)$ transitions

$$\alpha_{vJv'J+1}=\frac{8\pi^3c^4K_{vv'}}{3kT(2\pi kT/M)^{1/2}}(J+1)\left[N_vB_v\exp\left(-F_v(J)\frac{hc}{kT}\right)-N_vB_{v'}\exp\left(-F_{v'}(J+1)\frac{hc}{kT}\right)\right]. \quad (7)$$

[22] R. Herman and R. F. Wallis, J. Chem. Phys. 23, 637 (1955).
[23] $K_{vv'}$ is often denoted as $|R_{vv'}|^2$.

(b) For R-branch rotational transitions, i.e., for $R(J\text{-}1)$ transitions

$$\alpha_{vJv'J-1}=\frac{8\pi^3c^4K_{vv'}}{3kT(2\pi kT/M)^{1/2}}(J)\left[N_vB_v\exp\left(-F_v(J)\frac{hc}{kT}\right)-N_{v'}B_{v'}\exp\left(-F_{v'}(J-1)\frac{hc}{hT}\right)\right]. \quad (8)$$

For the purposes of analysis it is convenient to plot the α's for various parameters. We will normalize the α's to

$$\frac{8\pi^3c^4K_{vv'}}{3k(2\pi k/M)^{1/2}}N_{v'}.$$

Figures 5–9 show the α for $P(J+1)$ and $R(J-1)$ for $T=100°$K, 200°K, 300°K, 400°K, 500°K, for $N_v/N_{v'}=0.8$, 0.9, 1.0, 1.1, and 1.2 as a function of the *upper level* J. These are shown for the 7-6 brand vibrational-rotational transitions of CO. We see from these plots that it is definitely profitable to keep the T as low as possible. Also, the J position of maximum gain can be shifted by changing temperature and the $N_v/N_{v'}$. It is obvious from the figures why only P-branch rotational transitions have been seen in laser oscillation for CO. The R branch does not show gain until $N_v/N_{v'}\geq 1.00$ and even then, the gain on an R branch transition, starting from the same upper level J as a P-branch rotational transition, is always lower than that on the P-branch transition. This leads to competition between the two; the P branch starts oscillating first, and then inhibits the oscillation on the R branch transition. Again the rotational equilibrium within a vibrational level (i.e., Boltzmann equilibrium between the rotational levels) is very rapid ($\sim 10^{-6}$-10^{-7} sec)[24] compared to the average radiative lifetime of vibrationally excited levels of CO ($\sim 10^{-3}$ sec). Thus, it will be difficult to predict if an R-branch transition will show oscillation even though the P-branch transition starting from the same upper level J is not oscillating. Also, it is seen clearly that regardless of the temperature, P branch rotational transitions show gain even when there is no actual population inversion between the vibrational level population densities, i.e., for $N_v/N_{v'}<1$ or for T_v (vibrational temperature) positive.

To show the effect of variation of rotational (and molecular) temperature and $N_v/N_{v'}$ (or vibrational temperature) we show in Fig. 10 the position of maximum gain on P-branch rotational transitions, i.e., J for $\alpha_{vJv'J+1}$ maximum and positive as a function of $N_v/N_{v'}$ for various T. In Fig. 11 we show the peak gain on the P branch rotational transition having the maximum gain (see Fig. 10) as a function of $N_v/N_{v'}$ for various T, and in Figs. 12 and 13 we show the same data as in Figs. 10 and 11 but as a function of T for various $N_v/N_{v'}$.

Thus, it is seen that changing of $N_v/N_{v'}$ not only changes the maximum gain (Figs. 11 and 13) but also the position (in J and also obviously in frequency) of the maximum gain—or alternatively keeping $N_v/N_{v'}$ constant, a change in temperature makes a change in the position and amplitude of maximum-gain transition. Hence these two variables can be successfully used for "tuning" the laser so that a given transition will have the maximum gain.

Applying this analysis to the experimental data in Table I, we see from Fig. 10 that for an assumed $T=400°$K (in a dc discharge in atomic gases, $T\approx 400°$K) we find that $N_v/N_{v'}$ for the 10-9, 9-8, 8-7, 7-6, and 6-5 bands should be ≈ 1.00 or slightly less. If the delay between the current pulse and laser output pulse results in cooling off of the CO molecules, $T<400°$K and we see from Fig. 10 that $N_v/N_{v'}\approx 0.9$-1.0 for $300°\text{K}<T<400°$K. Under these circumstances, R-branch rota-

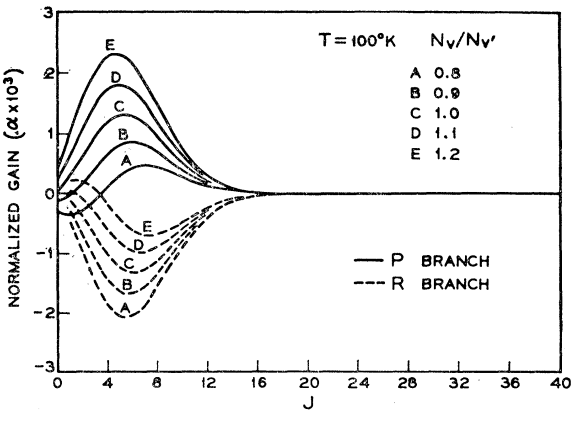

FIG. 5. Normalized $\alpha_{P(J+1)}$ and $\alpha_{R(J-1)}$ for 7-6 vibrational-rotational band of CO plotted as a function of *upper level* J for $T=100°$K and $N_v/N_{v'}=0.8$, 0.9, 1.0, 1.1, and 1.2.

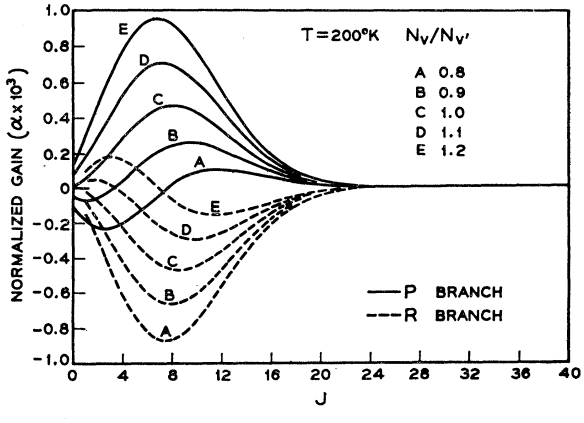

FIG. 6. Normalized $\alpha_{P(J+1)}$ and $\alpha_{R(J-1)}$ for 7-6 vibrational-rotational band of CO plotted as a function of *upper level* J for $T=200°$K and $N_v/N_{v'}=0.8$, 0.9, 1.0, 1.1, and 1.2.

[24] K. F. Herzfeld and T. A. Litowitz, *Absorption and Dispersion of Ultrasonics* (Academic Press Inc., New York, 1959).

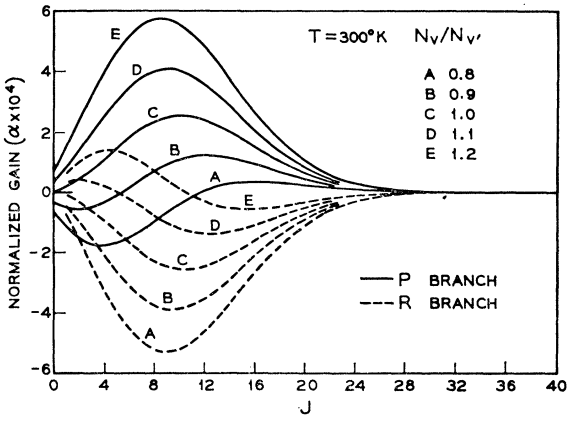

FIG. 7. Normalized $\alpha_{P(J+1)}$ and $\alpha_{R(J-1)}$ for 7-6 vibrational-rotational band of CO, plotted as a function of *upper level* J for $T=300°K$ and $N_v/N_{v'}=0.8$, 0.9, 1.0, 1.1, and 1.2.

tional transitions do not even show gain and thus the absence of laser oscillation on R branch rotational transitions is justified.

V. DISCUSSION OF EXCITATION MECHANISMS

In Sec. III we saw that the laser output was delayed after the excitation current pulse by 60–150 μsec depending upon the vibrational band. Time dependence

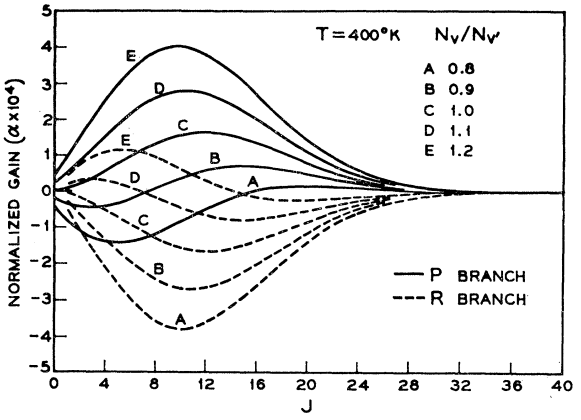

FIG. 8. Normalized $\alpha_{P(J+1)}$ and $\alpha_{R(J-1)}$ for 7-6 vibrational-rotational band of CO, plotted as a function of *upper level* J for $T=400°K$ and $N_v/N_{v'}=0.8$, 0.9, 1.0, 1.1, and 1.2.

analysis has been used to examine some of the possible excitation mechanisms reponsible for the CO vibrational-rotational laser. The long delay after the application of the excitation pulse implies very strongly that no direct excitation of CO molecules from the ground electronic state $v=0$ level to these higher vibrational levels can be a predominant mechanism. To look at other excitation processes we looked at the Angstrom band ($B^1\Sigma \rightarrow A^1\Pi$) radiation emitted from the side of the laser tube. Figure 14 shows an oscilloscope photograph of the voltage and current pulses together with the 4835 Å light output pulse from the side of the tube. (4835 Å radiation corresponds to the $0 \rightarrow 1$ band head of the $B^1\Sigma$-$A^1\Pi$ system.) The radiation was isolated by using a 250-mm Bausch and Lomb monochromator.

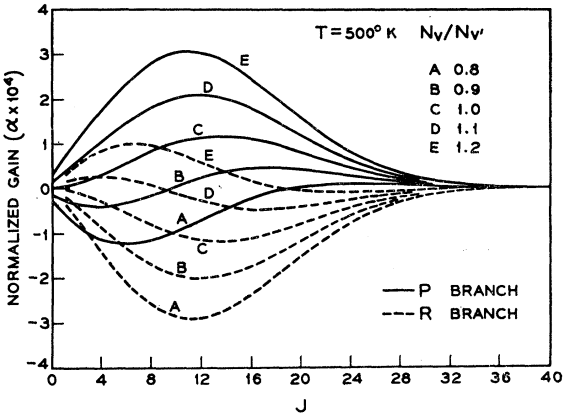

FIG. 9. Normalized $\alpha_{P(J+1)}$ and $\alpha_{R(J-1)}$ for 7-6 vibrational-rotational band of CO plotted as a function of *upper level* J for $T=500°K$ and $N_v/N_{v'}=0.8$, 0.9, 1.0, 1.1, and 1.2.

(Other bands in the angstrom system show similar time dependence.) We see that there is very little delay between the current pulse and the 4835-Å output pulse. This is indicative of direct electron impact excitation of the CO molecule to the $B^1\Sigma$. (This is also found by Cheo

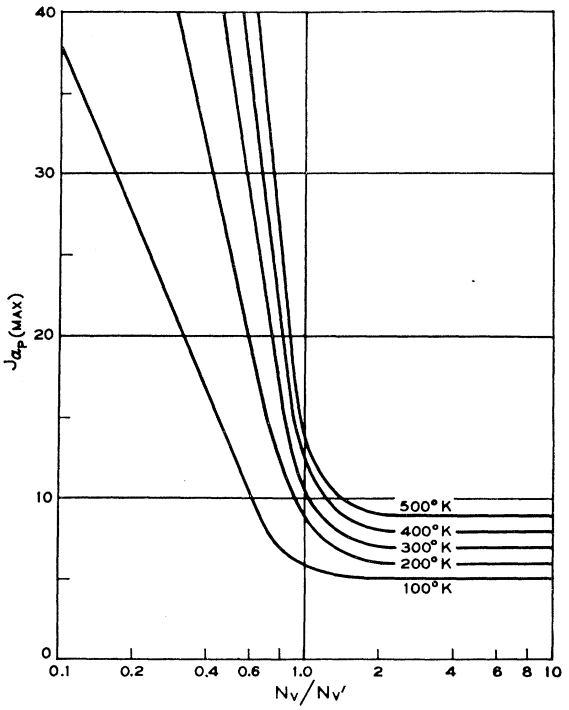

FIG. 10. J (of the upper level) for the maximum gain P branch transition of the 7-6 band of CO as a function of $N_v/N_{v'}$ for $T=100$, 200, 300, 400, and 500°K.

TABLE III. Calculated lifetimes for $v=10$ to $v=1$ vibrational levels of $X^1\Sigma^+$ state of CO together with constants used in calculations.

v	$\nu_{v\to v-1}$ (cm^{-1})	$R_{v\to v-1}$ (Ref. 26)	$A_{v\to v-1}$ (sec^{-1})	$\nu_{v\to v-2}$ (cm^{-1})	$R_{v\to v-2}$ (Ref. 26)	$A_{v\to v-2}$ (sec^{-1})	$\Sigma A_v=A_{v\to v-1}+A_{v\to v-2}$ (sec^{-1})	$\tau_v=1/\Sigma A_v$ (sec)
10	1907	...	...	3840	...	...	250 (Est.)	4.0×10^{-3} (Est.)
9	1933	3.110	215.2	3892	0.3084	17.25	232.45	4.302×10^{-3}
8	1959	2.923	197.8	3944	0.2696	13.72	211.52	4.73×10^{-3}
7	1985	2.721	178.5	3996	0.2312	10.50	189.00	5.291×10^{-3}
6	2011	2.508	157.7	4048	0.1936	7.66	165.36	6.047×10^{-3}
5	2037	2.278	134.8	4101	0.1566	5.20	140.00	7.142×10^{-3}
4	2064	2.028	111.2	4154	0.1202	3.21	114.41	8.740×10^{-3}
3	2090	1.784	89.66	4206	0.08417	1.62	91.28	10.955×10^{-3}
2	2116	1.421	59.33	4259	0.04814	0.55	59.88	16.70×10^{-3}
1	2143	1.000	30.30	...	...	...	30.30	33.0×10^{-3}

and Cooper[25] in their experiments on the CO electronic laser transitions of the angstrom band.) Thus it seems that the radiative decay of CO molecules from the $A^1\Pi$ state to various vibrational levels of the ground electronic state $X^1\Sigma^+$ probably constitutes the main excitation process responsible. The direct electron-impact excitation cross section is quite small as reported by Schulz.[12] From his data, it can be seen that it is possible that the electronic impact excitation can be effective through a compound state of CO located at about 2.2 eV.

Table III shows calculated vibrational-transition probabilities from the calculated ratios of matrix elements for various vibrational transitions as obtained by Cashion.[26] We have calculated the spontaneous emission transition probabilities for $v\to v-1$ and $v\to v-2$ transitions using the known value of $A_{1\to0}$ of 33 sec^{-1} (see for example, Ref. 5), with the following relation

$$A_{v\to v'}=\left(\frac{\nu_{v\to v'}}{\nu_{1\to0}}\right)^3\frac{|R_{v\to v'}|^2}{|R_{1\to0}|^2}A_{1\to0}. \tag{9}$$

$R_{v\to v'}/R_{1\to0}$ are given in Ref. 26. In Table III we also show the band center frequencies for $v\to v-1$ and $v\to v-2$ vibrational bands. We have assumed that these are the only two bands which contribute toward the radiative lifetime of the level v. With this assumption, Table III also shows the calculated lifetimes for levels up to $v=10$. ($v=1$ level lifetime is measured value as mentioned above.) With these lifetimes and spontaneous emission transition probabilities, we can write down the rate equations for the vibrational level population densities. We have assumed here that there is no laser action to change the radiative lifetimes and no significant deactivation of vibrationally excited CO ground electronic state molecules through collisions. The second of the assumptions has been shown to be valid at low CO pressures.[13] (The deactivation due to collisions whereby translational-vibrational energy exchange takes place has been shown to be a very slow process for a number of other molecules also.)[13,14] We also assume that the rotational-translational relaxation is very much faster compared to the radiative decay of

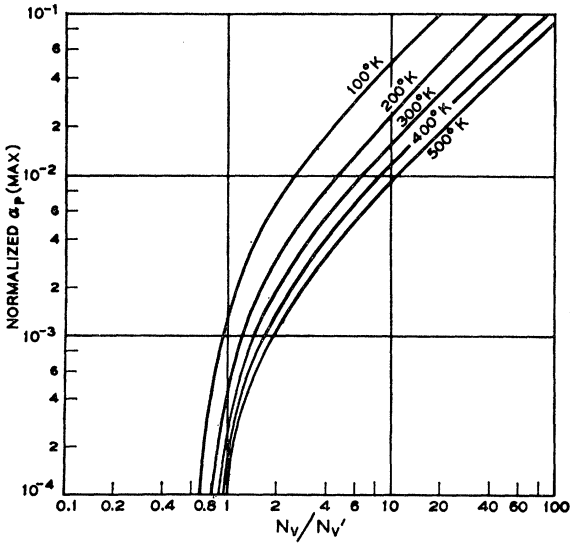

FIG. 11. Maximum α_{vJvJ+1}, for 7-6 band of CO as a function of $N_v/N_{v'}$ for $T=100$, 200, 300, 400, and 500°K.

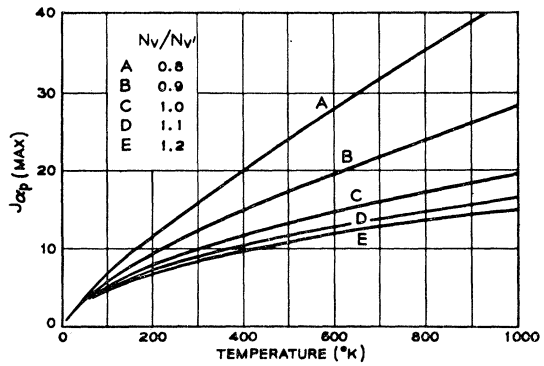

FIG. 12. J (of the upper level) for the maximum gain P branch transition of the 7-6 band of CO as a function of T for $N_v/N_{v'}=0.8$, 0.9, 1.0, 1.1, and 1.2.

[25] P. K. Cheo and H. G. Copper, Appl. Phys. Letters **5**, 42 (1964); H. G. Cooper and P. K. Cheo, Appl. Phys. Letters **5**, 44 (1964).

[26] K. Cashion, J. Mol. Spectry. **10**, 182 (1963).

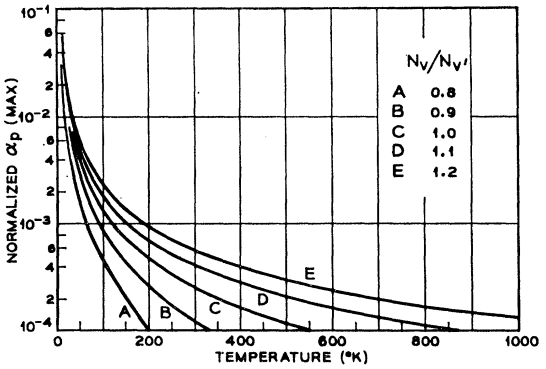

FIG. 13. Maximum $\alpha_{vJv'J+1}$ for 7-6 band of CO as a function of T for $N_v/N_{v'}=0.8$, 0.9, 1.0, 1.1, and 1.2.

the CO vibrationally excited molecules, i.e., we assume that the thermalization time required to obtain a Boltzmann distribution of molecules in various rotational levels of a vibrational level is very much shorter compared to the radiative lifetime of the molecules. This is seen to be true even at pressures as low as 0.1–1 Torr where $\tau_{\text{thermalization}}\approx 10^{-6}$-$10^{-7}$ sec (see Herzfeld and Litowitz[24] for a discussion on this subject) which is very much shorter than the radiative lifetime of the CO vibrational levels shown in Table III. Thus we can assign a single lifetime to all the rotational levels of a vibrational level.

With these assumptions the rate equations can be written as

$$\dot{N}_v = n_v + N_{v+1}A_{v+1\to v} + N_{v+2}A_{v+2\to v} - N_v(A_{v\to v-1}+A_{v\to v-2}). \quad (10)$$

Here $\dot{N}_v$ = time rate of change of population density N_v of vth vibrational level; n_v = excitation of molecules (rate) to vth vibrational level excluding the process of radiative cascade from the $v+1$ and $v+2$ vibrational levels. Here, as before, we have neglected all radiative transitions other than those which involve $\Delta v=1$ and 2. Solution of equations of these types for $v=1, 2, \cdots, 10$ with appropriate initial or excitation conditions will show the population densities of each of the vibrational levels as a function of time. For illustration we will solve these rate equations for three different sets of conditions.

1. cw case with selective excitation into $v=10$ level only, i.e., $n_{10}=$ constant and $n_9=n_8, \cdots, n_1=0$. This is the simplest case to analyze, and Figs. 15 and 16 show N_v and N_v-N_{v-1}, respectively, as a function of time starting at $t=0$ when $N_v=0$, and at $t=0$ the selective excitation begins. We see that under cw conditions no actual inversion can exist between vibrational levels, but we have seen from the earlier section that even in this case P-branch rotational transitions can oscillate. In Table IV we give the steady-state relative population densities of the ten vibrational levels. Also listed are the transitions which are expected to have the largest optical gain for each one of the bands, assuming a

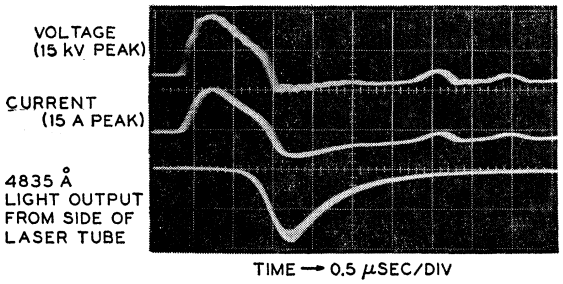

FIG. 14. Oscilloscope trace of pulse voltage, pulse current and 4835 Å light output from the side of the laser tube corresponding to the $0\to 1$ band head of the $B^1\Sigma$-$A^1\Pi$ system of CO.

molecular temperature of about 400°K. (To repeat, we have not included stimulated emission in the formulation of our rate equations.) Table IV shows the transitions which are most likely to be seen in laser oscillation assuming the stimulated emission does not significantly alter the radiative decay rates. Selective excitation of this type can be accomplished through energy transfer from another excited species of atoms or mole-

TABLE IV. Relative population densities N_v/N_{v-1} assuming a selective excitation of molecules to $v=10$ level, together with transitions expected to show maximum gain at $T_{\text{rot}}=400$°K.

v	N_v/N_{v-1}	Transition for maximum gain ($T=400$°K)
10	0.93	$P_{10\text{-}9}(14)$
9	0.91	$P_{9\text{-}8}(14)$
8	0.89	$P_{8\text{-}7}(15)$
7	0.875	$P_{7\text{-}6}(16)$
6	0.845	$P_{6\text{-}5}(17)$
5	0.82	$P_{5\text{-}4}(19)$
4	0.795	$P_{4\text{-}3}(21)$
3	0.66	$P_{3\text{-}2}(31)$
2	0.50	$P_{2\text{-}1}(50)$

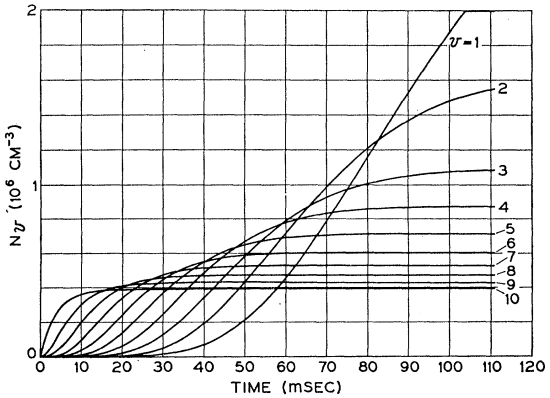

FIG. 15. N_v as a function of time, calculated for cw operation with $N_v=0$ at $T=0$ and $n_{10}=10^8$ sec^{-1} cm^{-3} with $n_{v\leq 9}=0$ (see text).

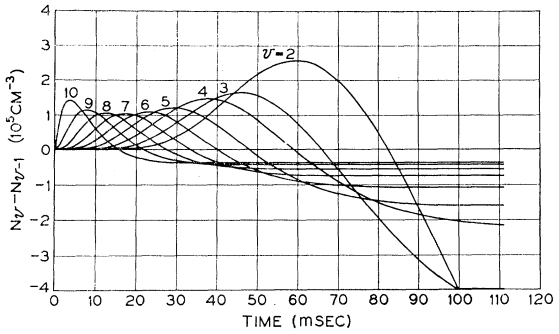

FIG. 16. N_v-N_{v-1} as a function of time for the same initial conditions as in Fig. 15.

cules. One such suggested example is the use of Hg($^3P_{0,1,2}$) states.[27] It is not entirely clear, however, if such a transfer will produce enough selective excitation to obtain laser oscillation.

2. Pulsed operation: At $t=0$, all $N_v=N$, and no further excitation n_v takes place. Figures 17 and 18

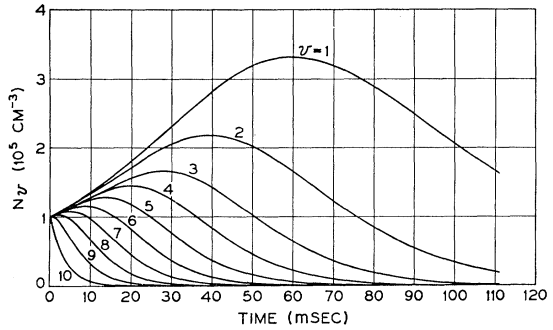

FIG. 17. N_v as a function of time, calculated for pulsed operation with $N_v=10^5$ cm^{-3} at $t=0$ and $n_v=0$ (see text).

show the behavior of population densities of the $v=10$, $\cdots$, 1 levels as a function of time. Here at $t=0$, $N_v/N_{v-1}=1$ and laser oscillation should start immediately on $P(11)$ transitions (see previous section). However, now the ratios N_v/N_{v-1} are changing and the

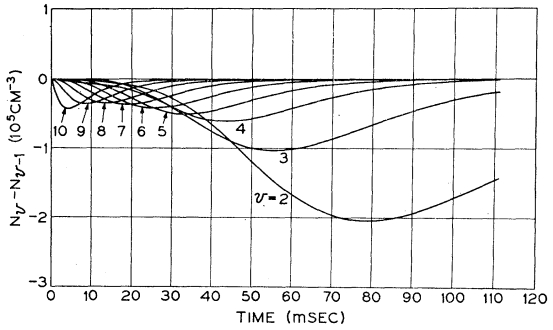

FIG. 18. N_v-N_{v-1} as a function of time for the same initial conditions as in Fig. 17.

[27] J. C. Polanyi, Appl. Opt. Suppl. Chemical Lasers, 109 (1965).

P-branch rotational transition having the maximum gain shifts toward higher J values with accompanied decrease in the maximum gain. Experimental findings do not corroborate this. As seen from Table I there are various amounts of delay involved before each band starts oscillating. According to the analysis with the stated initial conditions, oscillation should have started

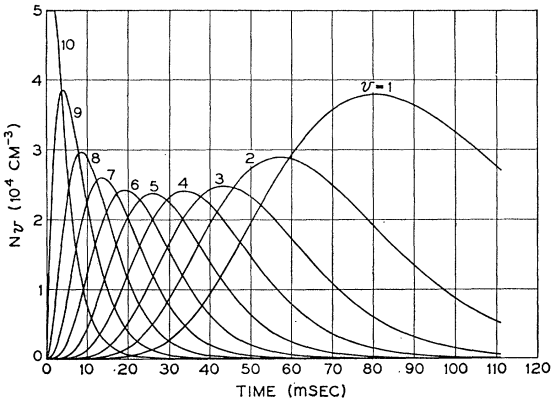

FIG. 19. N_v as a function of time for pulsed operation with $N_{v\leq 9}=0$, and $N_{10}=10^5$ cm^{-3} at $t=0$ (see text).

at $t=0$, i.e., right after the excitation pulse if all the vibrational levels were equally populatd. Also that the, gain at $t=0$ is the maximum as seen from Fig. 11 because for $t>0$, $N_v/N_{v'-1}$ becomes smaller and smaller with an accompanied decrease in the population densities.

3. Pulsed operation: At $t<0$, all $N_v=0$, and at $t=0$, a finite fixed number of molecules are excited to

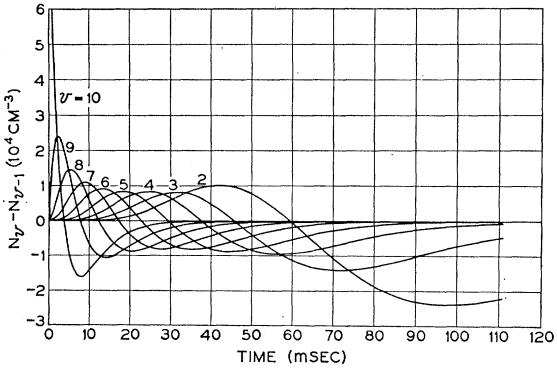

FIG. 20. N_v-N_{v-1} as a function of time for the same initial conditions as in Fig. 19.

the $v=10$ level in a time short compared to the lifetime of the $v=10$ level. Thus we can take, $N_{9,8,\ldots,1}=0$ and $N_{10}=10^5$, say, at $t=0$. Figure 19 shows the population densities as a function of time. We also show in Fig. 20 the N_v-N_{v-1} as a function of time, and now we see that first the 10-9 band starts oscillating, then 9-8, 8-7 and so on. Except for the 10-9 band, there are finite

time delays involved for possible laser oscillation on 8-7, 7-6, ···, 2-1 bands. The population inversion travels down the vibrational level ladder in the form of a wave, i.e., first the 10-9 band is inverted, then the 9-8, 8-7 and so on.

This trend, however, is in a direction opposite to the experimentally determined delays. We see from Table I that the 6-5 band starts oscillating first, then the 7-6 and so on, and 10-9 oscillates last, i.e., the disturbance caused by laser oscillation travels upward to cause inversion. Also we see that the analysis with these assumptions predicts that inversion should also be established between the 5-4, 4-3, ···, 2-1 levels at longer times, which is not found to be the case in experimental investigations. No laser action was detected for vibrational levels $v<5$. In light of the three simple cases analyzed and the experimental findings, we have to conclude that the excitation conditions are not as simple as those described in (2) and (3) even under pulsed operation. The levels $v<5$ are populated very heavily so that no laser oscillation takes place on P branch rotational transitions for these bands with $v<5$. In the above two pulsed operation examples, it was seen the J for maximum gain on a P-branch rotational transition shifts with time. This is not borne out by experimental findings. This implies that presumably with a given vibrational band, different rotational transitions oscillate at different times. But, experimentally, it was seen that *all* the rotational transitions belonging to one vibrational band started oscillating approximately at the same time. This also implies complicated and time-dependent excitation processes n_v which may involve recombination in addition to cascading from higher electronic levels.

ACKNOWLEDGMENTS

The author thanks R. J. Kerl for excellent technical assistance and Mrs. C. A. Lambert for aid in computer calculations.

PHYSICAL REVIEW VOLUME 141, NUMBER 1 JANUARY 1966

Excitation-Transfer Collisions between Rubidium and Helium Atoms

T. J. BEAHN, W. J. CONDELL, AND H. I. MANDELBERG
Laboratory for Physical Sciences, 7338 Baltimore Avenue, College Park, Maryland
(Received 10 June 1965; revised manuscript received 2 September 1965)

An experiment is described which measures the collision cross section for transfer of excitation in rubidium by helium. Rubidium atoms are pumped to either the $^2P_{1/2}$ or $^2P_{3/2}$ state by irradiation with one of the resonance lines. Some excited rubidium atoms are transferred to the other P state by collisions with helium atoms. The rubidium atoms then radiate both resonance lines. Measurements of the intensities of both resonance lines as a function of helium pressure are used to calculate the collision cross section. The cross section for $^2P_{1/2}$ to $^2P_{3/2}$ is 1.0×10^{-17} cm$^2\pm10\%$ and for $^2P_{3/2}$ to $^2P_{1/2}$ is 1.2×10^{-17} cm$^2\pm10\%$.

I. INTRODUCTION

THE effect of rare-gas collisions with sodium atoms excited to the $^2P_{1/2}$ or $^2P_{3/2}$ states was first observed by Wood.[1] Subsequently, Lochte-Holtgreven[2] repeated Wood's experiments, and from his data cross sections for the transfer between the two states by rare gases can be found. More recently, similar work has been done by Seiwert,[3] Jordan,[4] and by Krause and his co-workers.[5,6] Recent interest in optical pumping of rubidium in rare-gas buffered cells as well as interest in the fundamental processes involved prompted us to examine the interaction of excited rubidium atoms with helium.

Rubidium is particularly well suited for such investigation because it has sufficient vapor pressure at easily attained temperatures and the resonance lines, lying at 7800 and 7947 Å, are easily isolated with interference filters.

If rubidium vapor is irradiated with D_1 radiation (7947 Å) from a rubidium light source, it will in the presence of helium gas reradiate not only D_1 light but also D_2 (7800 Å). The relative amount of D_2 will depend on the amount of helium gas present. By varying the amount of helium gas, we can find a collision cross section for the transfer from $^2P_{1/2}$ to $^2P_{3/2}$. Similarly, if the rubidium vapor is irradiated with D_2 light, it will reradiate D_1 in addition to D_2 because of the collisions with helium. Again, by varying the amount of helium present we can find the cross section for the transfer $^2P_{3/2}$ to $^2P_{1/2}$. The transfer can also be caused by the excited rubidium atom colliding with a ground-state

[1] R. W. Wood, Phil. Mag. 27, 1018 (1914).
[2] W. Lochte-Holtgreven, Z. Physik 47, 362 (1928).
[3] R. Seiwert, Ann. Physik 18, 54 (1956).
[4] J. A. Jordan, Ph.D. thesis, University of Michigan, 1964 (unpublished).
[5] G. D. Chapman and L. Krause, Can. J. Phys. 43, 563 (1965).
[6] G. D. Chapman, M. Czajkowski, A. G. A. Rae, and L. Krause, Abstracts of the IVth International Conference on the Physics of Electronic and Atomic Collisions; Quebec, Canada, 1965, p. 55 (unpublished).

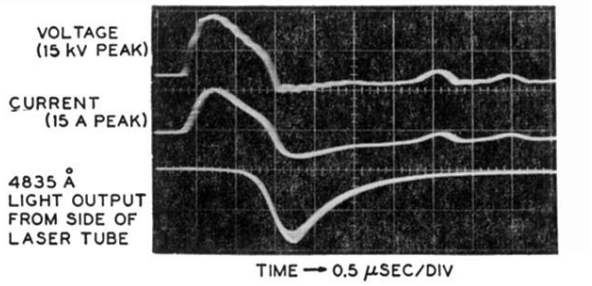

FIG. 14. Oscilloscope trace of pulse voltage, pulse current and 4835 Å light output from the side of the laser tube corresponding to the $0 \rightarrow 1$ band head of the $B^1\Sigma$-$A^1\Pi$ system of CO.

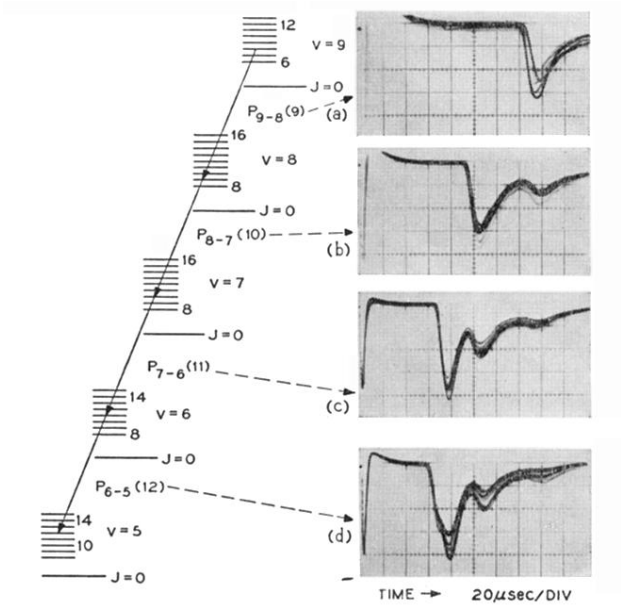

FIG. 4. Laser pulses showing cascade nature of CO laser transitions described in Eq. (2): (a) $P_{9\text{-}8}(9)$ at 5.26310 μ, (b) $P_{8\text{-}7}(10)$ at 5.20345 μ, (c) $P_{7\text{-}6}(11)$ at 5.14530 μ, and (d) $P_{6\text{-}5}(12)$ at 5.08845 μ. (Energy-level diagram, not to scale, is shown on the left. In each of the oscilloscope traces, the current pulse occurs at the left-hand edge.)